文章编号: 1001 - 9014(2016)01 - 0011 - 04

DOI:10.11972/j.issn.1001 - 9014.2016.01.003

Tunable broad stop-band filter based on multilayer metamaterials in the THz regime

ZHONG Min[1,2*], HAN Gui-Ming[3]

(1. Department of Physics, Nanjing Normal University, Nanjing 210023, China; 2. Hezhou College, Hezhou 542899, China;
3. Institute of Information and Technology, Guilin University of Electronic Technology, Gulin 541004, China)

Abstract: A periodic multilayer structure with metal and dielectric layers is proposed to obtain a broad stop-band filter. The influence of three factors (the number of the metal layer (n), the metal layer and the dielectric layer) on the stop-band and central frequency of cross ring resonator (CRR) filter has been investigated. Simulated results indicate that the stop-bandwidth can reach to 2.2THz. Moreover, The stop-band and central frequency can be modulated by selecting appropriate n or dielectric layer, but it is not sensitive to the metal layer.

Key words: filter, metamaterials, stop-band, transmission

PACS: 41. 20. Jb, 78. 20. Cj, 73. 20. Mf, 42. 25. Bs

调制太赫兹范围的多层超材料大带宽阻带过滤器

钟 敏[1,2*], 韩贵明[3]

(1. 南京师范大学 物理与科学技术学院,江苏 南京 210023;2. 贺州学院,广西 贺州 542899;
3. 桂林电子科技大学信息科技信息科技学院,广西 桂林 541004)

摘要:设计了金属和介电层的周期性多层结构的大带宽阻带过滤器. 三个因素(金属层数,金属层和介电层)对CRR结构的过滤器的阻带和阻带中心频率的影响进行了研究. 模拟结果表明阻带带宽可以达到2.2 THz. 同时,阻带和中心频率可以通过选择合适的金属层数或者介电层来调制,但它们对金属层的种类并不敏感.

关 键 词:过滤器;超材料;阻带;透射率

中图分类号:0431 **文献标识码**:A

Introduction

Metamaterials have attracted a great deal of attention during the past few years, because of their potential applications, including perfect absorbers[1], perfect lens[2], imaging[3], invisibility cloaks[4], sensing[5] and filters[6]. These metamaterials are typically made up of two or more structured metallic layers which are separated with dielectric layers, either free standing or supporting by a suitable substrate. Among these devices, stop-band filter in the THz regime attracts a great attention[7], which is designed to ensure high tolerances well to frequency operations or filter specific frequencies of wave propagating. However, many stop-band filters can't scale well in the THz region because of their resonant bandwidth is too narrow, which significantly limits these stop-band filters application demanding for effectively filtering broadband radiation. Recently, a novel design for a tunable broad stop-band filter has been presented[8]. There are three resonance modes in a stop-band. However, it must use three or more metal layers to get a 1.0THz bandwidth, which is not conductive to miniaturization and cost reduction. It is important that designing and providing a filter with a broad stop-band in the THz region. For instance, a filter can be fabricated practical, with high-efficiency broad stop-band, would be found applications in screening of radiant energy, using as the terminator of energy harvesting devices, and so on. Motivated by these reasons, a cross-circle structure is de-

Received date: 2015 - 01 - 21, **revised date**: 2015 - 02 - 16 **收稿日期**:2015 - 01 - 21, **修回日期**:2015 - 02 - 16

Foundation items: Supported in part by the and Graduate Research and Innovation Program of ordinary university of Jiangsu (CXLX13_390), Doctor's Scientific research foundation of Hezhou University (HZUBS201503).

Biography: ZHONG Min (1984-), man, Guangxi Hezhou, master. Research area involves metamaterials. E-mail: zhongmin2012hy@163.com

* **Corresponding author**: E-mail: zhongmin2012hy@163.com

signed whose stop-bandwidth and central frequency can be tunable in the THz region. And there is only one resonance mode in stop-band, just use two metal layers to get a 1.4 THz bandwidth. The filter can be operated to select bandwidth in the THz regime and provide a desirable filtering method.

1 Design of CRR Structure Filter

A unit cell of the cross ring resonator (CRR) is illustrated in Fig. 1. The multilayer microstructure consists of two aluminum layers and one dielectric layer. The dielectric layer is selected as SU-8. And dimensional parameters are: $P = 65\mu m$, $L = 60\mu m$, $R = 12\mu m$, $w = 26\mu m$, $t_1 = 0.1$, $t_2 = 12$.

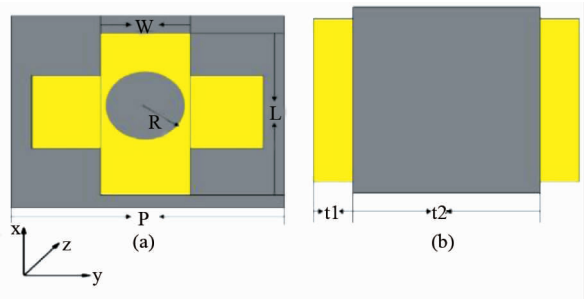

Fig. 1 (a) Top view of a unit cell of the CRR structure filter; (b) side view of the unit cell of the CRR structure filter for $n = 2$. The yellow part is metal layer, and the grey part is dielectric layer

图1 (a)CRR结构单元的俯视图,(b)CRR结构单元的侧视图(以 $n = 2$ 为例),其中,黄色部分为金属层,灰色部分为介质层

To find out the potential physics behind the stop-band, the commercial software Ansoft HFSS13.0 is employed. In our simulation, the dielectric constant of SU-8 is[9] and the Drude model is used to describe the dielectric constant of the aluminum layer:

$$\varepsilon(\omega) = 1 - \frac{\omega_p^2}{\omega^2 - i\omega\gamma_D} \quad , \quad (1)$$

here, $\omega_p = 1.37 \times 10^{16} s^{-1}$ is the plasma frequency and $\gamma_D = 9 \times 10^{13} s^{-1}$ is the collision frequency[10], respectively. The aluminum layer is perfect electric conductor for metal in our simulation. The electric field is in the y axis(E) and the magnetic field is in the x axis(H). The polarized wave propagates along the z axis(k). Two ideal electric conductor planes have been used on the boundary normal to the y axis and two ideal magnetic conductor planes has been utilized on the boundary normal to the x axis[11]. The model is tested in air with light incident to the CRR structure.

2 Simulated results

Simulated transmission spectra with different number of aluminum layers (n) are shown in Fig. 2. A stop-band dip is observed in the transmission spectra with n increasing. For $n = 1$, the stop-band dip locals at $f_0 \approx 2.5$ THz, which corresponds to a single resonance model. The bandwidth of the dip is $\Delta f \approx 0.11$ THz. Here, Δf is the full stop-bandwidth and f_0 is the resonance frequency of the stop-band. A typical stop-band filter is obtained. However, the bandwidth of the filter ($n = 1$) is too narrow to prevent the filter from being used for filtering broadband radiation effectively. In order to expand the stop-bandwidth, n is increased. As shown in Fig 2(b) ~ (e), for $n = 2$, the stop-band is expanded to $\Delta f \approx 1.4$ THz. It means that a typical broad stop-band filter is obtained. For $n = 3$, $\Delta f \approx 1.6$ THz and the transmission spectrum consists of only one resonant mode, too. Similarly, for $n = 4$, and $n = 5$, the stop-bandwidth are $\Delta f \approx 2.0$ THz and $\Delta f \approx 2.2$ THz, respectively. The central frequency of stop-band is blue-shifted obviously with n increasing, see the dotted line in Fig. 2. Simulated results in Fig. 2 reveal that the number of metal layer has an important influence on the bandwidth and central frequency of stop-band of the CRR structure filter.

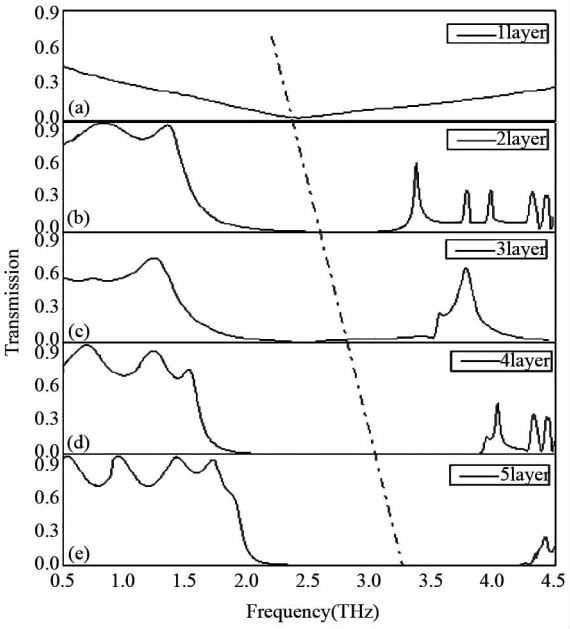

Fig. 2 Simulated transmittance spectra of the CRR structure with different number of aluminum layer: (a) $n = 1$; (b) $n = 2$; (c) $n = 3$; (d) $n = 4$; (e) $n = 5$

图2 不同数量铝层的CRR结构超材料滤波器的模拟透射谱: (a) $n = 1$; (b) $n = 2$; (c) $n = 3$; (d) $n = 4$; (e) $n = 5$

3 Discussion for CRR structure filter

To gain insight into the mechanisms which leads to the broad stop-band, the influence of the distribution of electric field on the broad stop-band has been studied in the near-field. On the one hand, the distribution of the electric fields is similar in each metal layer, while the intensity of the electric field is decreased from the upper layer to the lower layer, as illustrated in Fig. 3(a) ~ (c). On the other hand, the distribution of the electric field on the upper metal layer is investigated at different resonance frequencies, as shown in Fig. 3(d) ~ (f). To facilitate the study, at firstly, a resonance frequency

higher than the stop-band frequency regime, such as 4.15 THz, is selected to investigate the resonance mode. The resonance mode reveals a inward coupling between the circular hole when the resonance frequency higher than stop-band, as shown in Fig. 3(d). Then, select a lower resonance frequency, such as 1.1THz. As shown in Fig. 3(f), the resonance mode exhibits a strongly coupling between two adjacent unit cells. Finally, a resonance frequency in the stop-band frequency regime, such as 2.75 THz, is selected and simulated. These resonance modes which are discussed above exhibit a plasmonic hybridization obviously, as shown in Fig. 3(e), and these two coupling resonance modes are obviously strengthened because of the enhanced capacitance of CRR structure. At the same time, the distribution of current in different metal layers is investigated. As shown in Fig. 4(a) ~ (c), the intensity of the current is decreased from the upper layer to the lower layer, which is the same as the resonance intensity of the near-field electric field. When the resonance frequency is in the range of the stop-band, the intensity of the distribution of current is significantly higher than the frequency outside the stop-band. Through comparing Fig. 2, 3, 4, it can be found that the intensified capacitance of CRR structure leads to the stop-band of filter broader. The resonance between circular hole and the resonance between two adjacent unit cells has an important influence on bandwidth and central frequency of the stop-band.

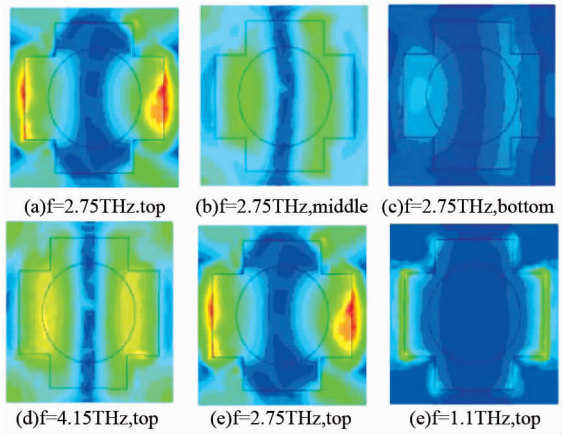

Fig. 3　(a) ~ (c) Simulated distributions of the electric field in the top, middle, and underneath layers at the frequency of 2.75 THz. (d) ~ (e) Simulated distributions of the electric field in the top layer of CRR structure at frequency of 4.15, 2.75, and1.1 THz
图 3　(a) ~ (c)共振频率为 2.75 THz 时在顶层、中间层和底层金属层上分布的模拟电场强度;(d) ~ (e)共振频率为 4.15 THz, 2.75 THz 和 1.1 THz 时顶层金属层上的模拟电场强度

To evaluate the filter performance of the CRR structure, the quality factors (Q) is employed:

$$Q = f_0/\Delta f \quad , \quad (2)$$

In the formula (2), the lower the value of the quality factor, the broader the stop-band of the CRR structure filter is. As shown in Fig. 5, Q is decreased with n increasing. Such a broad stop-band filter can effectively eliminate the interfering signal or suppress the undesired

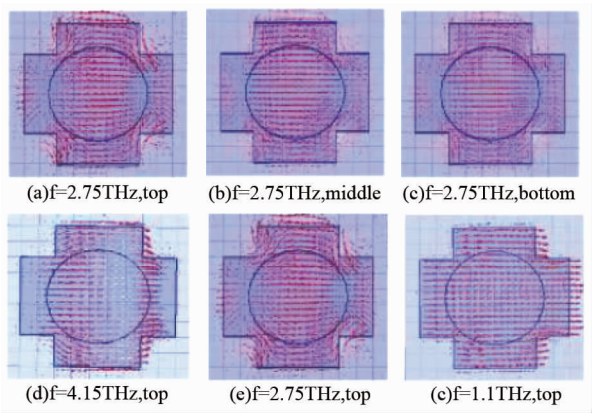

Fig. 4　(a) ~ (c) Simulated distributions of the current in the top, middle, and underneath layers at the frequency of 2.75 THz. (d) ~ (f) Simulated distributions of the current in the top layer at frequency of 4.15, 2.75, and 1.1 THz
图 4　(a) ~ (c)共振频率为 2.75 THz 时在顶层、中间层和底层金属层上分布的模拟电流强度;(d) ~ (e)共振频率为 4.15 THz, 2.75 THz 和 1.1 THz 时顶层金属层上的模拟电流强度

responses in the THz range.

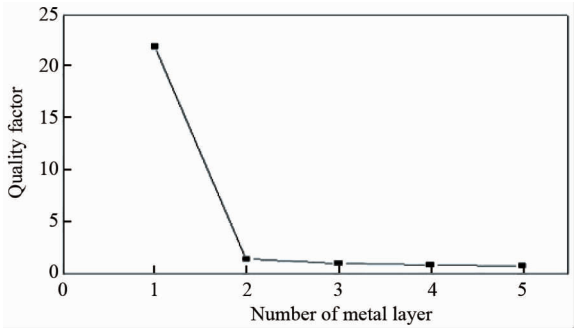

Fig. 5　Quality factor of CRR structure filter with the number of aluminum layers (n)
图 5　CRR 结构滤波器的金属层数量(n)与质量因子(Q)之间的关系图

The relationship between the metal layer, dielectric layer, and the stop-bandwidth is studied, as shown in Fig. 6. For $n = 2$, the metal layer has been changed to gold layer, copper layer and silver layer. Both central frequency and stop-band of these samples are very similar. However, the dielectric layer has an important influence on the central frequency and stop-band. In our simulation, the dielectric constant is reduced from 5 to 1, the stop-band is broaden and the central frequency blue-sifted obviously, as shown in Fig. 7. The CRR structure filter is sensitive to the dielectric layer but insensitive to the metal layer. Moreover, the multilayer electron-beam lithography technique can be used to manufacture this CRR structure[12]. It means that the fabrication of CRR structure filter is feasible and practical.

4　Conclusion

A broad stop-band metamaterials filter with CRR

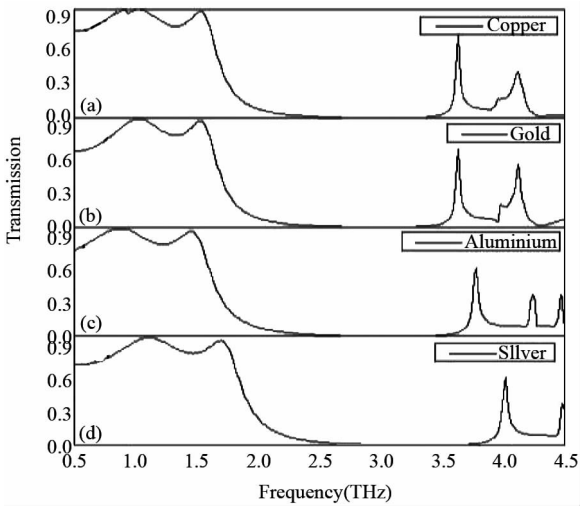

Fig. 6 Simulated transmission spectra of different metal layer with $n=2$

图6 不同种类金属层的模拟透射谱(以 $n=2$ 为例)

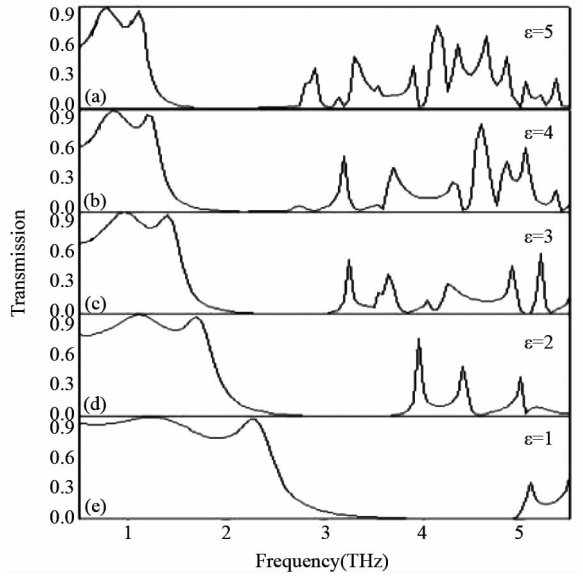

Fig. 7 Simulated transmission spectra of different dielectric constant with $n=2$

图7 不同种类介质层的模拟透射谱(以 $n=2$ 为例)

structure in the THz regime is designed and simulated. Results indicate that a broad stop-band filter is realized through using a multilayer structure consisting of alternating metal layers and dielectric layers. The plasmonic hybridization of inward coupling mode and adjacent unit cells coupling resonance mode leads to the stop-band broader. The stop-bandwidth can reach to 2.2THz with increasing the metal layer number. The stop-band filter is sensitive to the dielectric layer but insensitive to the metal layer. Moreover, the central frequency of stop-band is blue-shifted with n increasing or the dielectric constant of dielectric layer decreasing. A broad stop-band filter can be developed by selecting the appropriate structural parameters, and stacking CRR structure metal layers and dielectric layers.

References

[1] Alaee R, Farhat M, Rockstuhl C, *et al.* A perfect absorber made of a grapheme micro-ribbon metamaterial [J], *Optics Express.*, 2012, **20**: 28017-28024.

[2] Fang N, Lee H. Sun, C, *et al.* Sub-Diffraction-Limited Optical Imaging with a Silver Superlens [J], *Science.*, 2005, **308**:534-537.

[3] LIU Xu, Starr T. Starr A. F, *et al.* Phys. Rev. Lett. 2010, **104**: 207403-207407.

[4] Schuring D, Mock J J, Justice B J, *et al*, Metamaterial Electromagnetic Cloak at Microwave Frequencies [J], Science., vol. 314, pp. 977-981, 2006.

[5] LIU Na, Mesch M, Weiss T, *et al. NanoLett.* 2010, **10**: 2342-2348.

[6] Engheta N, Al'u A, *Filters and feedbacks in metamaterial nanocircuits, presented at the Photonic Metamaterials: From Random to Periodic* [M], Jackson Hole, WY, 2007, Paper ThA1.

[7] Chin J Y, Lu M, CUI Tie-Jun, Metamaterial polarizers by electric-field-coupled resonators [J], *Appl. Phys. Lett.*, 2008, **93**:251903-251905.

[8] LI Zhong-Yang, Yujie J. Ding, Broadband stopband filter for terahertz wave based on multi-layer metamaterial microstructure, [C], *Lasers and Electro-Optics (CLEO)*, Conference,2012.

[9] HUA YL, LI Z L, Analytic modal solution to transmission and collimation of light by one-dimensional nanostructured subwavelength metallic slits [J], *J. Appl. Phys.* 2009, **105**: 013104-013111.

[10] Smith D R, Vier D C, Konschny T, *et al.* Electromagnetic parameter retrieval from inhomogeneous metamaterials[J], *Phys. Rev. E*, 2005, **71**:036617-036627.

[11] Smith D R, Schultz S, Markos P, *et al.* Determination of effective permittivity and permeability of metamaterials from reflection and transmission coefficients[J], *Phys. Rev. B.*, 2002, **65**:195104-195108.

[12] Han N R, Chen Z C, Lim C S, *et al.* Broadband multi-layer terahertz metamaterials fabrication and characterization on flexible substrates [J], *Opt. Exp*, 2011, **19**:6990-6998.

(上接5页)

[20] Woltgens H, Friedrich I, Njorog W K, *et al.* Optical electrical and structural properties of Al-Ti and Al-Cr thin films [J]. *Thin Solid Films*, 2001, **388**: 237-244.

[21] Mookerji B, Stratman M, Wall M, *et al.* The optical constants of gallium stabilized δ-plutonium metal between 0.7 and 4.3 eV measured by spectroscopic ellipsometry using a double-windowed experimental chamber[J]. *Journal of Alloys and Compounds*, 2007, **444**: 339-341.

[22] Pells G P, Montgomery H. The optical properties of α-phase Cu-Zn, Cu-Ga, Cu-Ge and Cu-As alloys [J]. *Metal Physics Supplement*, 1970, **3**: s330.

[23] Palik E D. *Handbook of Optical Constants of Solids*[M]. Orlando: Academic Press, 1985.

[24] Wooten F. *Optical Properties of Solids*[M]. New York: Academic Press, 1972.

[25] Allen J W, Lucovsky G, Mikkelsen J C. Optical properties and electronic structure of crossroads material MnTe[J]. *Solid State Communications*, 1977, **24**(5): 367-370.

[26] Smith J B, Ehrenreich H. Frequency dependence of the optical relaxation time in metals[J]. *Physical Review B*, 1982, 25(2): 923.

[27] Thompson B V. Neutron Scattering by an Anharmonic Crystal [J]. *Physical Review*, 1963, **131**(4): 1420.

[28] Kim K J, Chen L Y, Lynch D W. Ellipsometric study of optical transitions in $Ag_{1-x}In_x$ alloys[J]. *Physical Review B*, 1988, **38**(18): 13107.

[29] O'Learya S K. An analytical density of states and joint density of states analysis of amorphous semiconductors[J]. *Journal of Applied Physics*, 2004, **96**(7): 3680.

[30] Liang W Y, Beal A R. A study of the optical joint density-of-states function[J]. *Solid State Physics*, 1976, **9**: 2824-2833.